nature nanotechnology

LETTERS

PUBLISHED ONLINE: 13 JUNE 2010 | DOI: 10.1038/NNANO.2010.111

Large oscillations of the magnetoresistance in nanopatterned high-temperature superconducting films

Ilya Sochnikov[1]*, Avner Shaulov[1], Yosef Yeshurun[1], Gennady Logvenov[2] and Ivan Božović[2]

Measurements on nanoscale structures constructed from high-temperature superconductors are expected to shed light on the origin of superconductivity in these materials[1–7]. To date, loops made from these compounds have had sizes of the order of hundreds of nanometres[8–11]. Here, we report the results of measurements on loops of $La_{1.84}Sr_{0.16}CuO_4$, a high-temperature superconductor that loses its resistance to electric currents when cooled below ~38 K, with dimensions down to tens of nanometres. We observe oscillations in the resistance of the loops as a function of the magnetic flux through the loops. The oscillations have a period of $h/2e$, and their amplitude is much larger than the amplitude of the resistance oscillations expected from the Little–Parks effect[12,13]. Moreover, unlike Little–Parks oscillations, which are caused by periodic changes in the superconducting transition temperature, the oscillations we observe are caused by periodic changes in the interaction between thermally excited moving vortices and the oscillating persistent current induced in the loops. However, despite the enhanced amplitude of these oscillations, we have not detected oscillations with a period of h/e, as recently predicted for nanoscale loops of superconductors with *d*-wave symmetry[1–6], or with a period of $h/4e$, as predicted for superconductors that exhibit stripes[7].

Molecular beam epitaxy (MBE) was used to synthesize 26-nm-thick films of optimally doped $La_{1.84}Sr_{0.16}CuO_4$ on single-crystal $LaSrAlO_4$ substrates polished perpendicular to the (001) direction[10,11]. The films were characterized *in situ* by reflection high-energy electron diffraction (RHEED), and *ex situ* by X-ray diffraction, atomic force microscopy and mutual inductance measurements. Subsequently, as detailed in the Methods, the films were patterned into a network of 'small' square loops, the sides of which were between 75 and 150 nm long, separated by 'large' square loops with sides of length 500 nm; the width of all features was ~25 nm. A typical network of small and large loops is shown in Fig. 1. The length and width of the small squares were almost an order of magnitude smaller than those in previously studied high-T_c networks and rings[8–11].

Figure 2 shows the magnetoresistance of the 150/500-nm network measured at $T = 28.4$ K in a magnetic field applied normal to the film surface (and to the *a*–*b* crystallographic plane). The measured magnetoresistance exhibits large oscillations superimposed on a parabolic-like background. The period of these oscillations, $H_0 \approx 950$ Oe, corresponds to the magnetic flux quantum, $\Phi_0 = h/2e = AH_0$, where h is Planck's constant, e the electron charge and A the area of the small loop. Oscillations with a period of ~80 Oe, which correspond to the large loops, are also observed, but their amplitude is too small to be noticed on the scale of Fig. 2.

The measured magnetoresistance, normalized to the normal-state resistance at $T = 30.2$ K, $R_n = 36\ \Omega$, is presented in Fig. 3a as a function of the temperature T and the applied magnetic field H. Periodic oscillations of R are observed for temperatures between 26 and 30.2 K. The temperature dependence of the amplitude of these oscillations is described by the diamonds in the inset to Fig. 2. Note that the field range in Fig. 3 is limited to low fields where the parabolic-like background is insignificant.

It is tempting to interpret these data as Little–Parks oscillations[8,12–17] originating from the periodic dependence of the critical temperature T_c on the magnetic field. However, the amplitude of the oscillations seen in Fig. 2 is much too large. Taking a typical value[18] for the coherence length in $La_{1.84}Sr_{0.16}CuO_4$

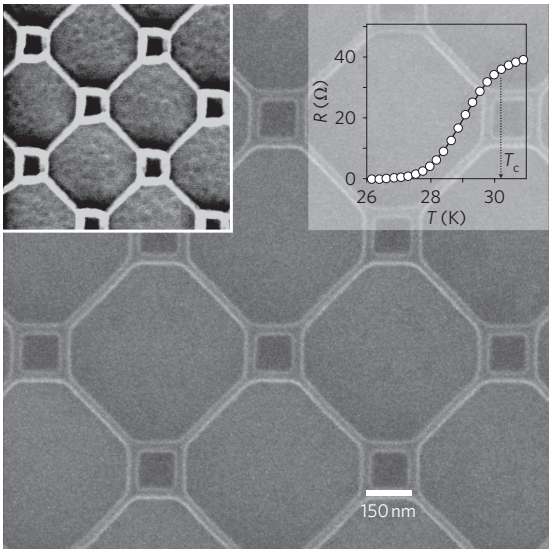

Figure 1 | Patterned superconducting film. Main panel: scanning electron microscope (SEM) image of a $La_{1.84}Sr_{0.16}CuO_4$ superconducting film covered with a patterned layer of poly(methyl methacrylate) (PMMA) resist (thin lines with bright edges). The left inset shows an SEM image of a part of the resulting superconducting network (150 × 150-nm^2 loops separated by 500 × 500-nm^2 loops) after the uncovered parts of the film were removed by ion milling. The right inset shows the measured (white circles) temperature dependence of the network (30 × 30 μm^2) resistance in zero magnetic field near the superconducting transition; the current is 1 μA. In the patterned film the onset temperature for superconductivity is 30.2 K and the transition width is ~2 K (compared with 38 K and ~0.5 K for the as-grown film).

[1]Department of Physics, Institute of Superconductivity and Institute of Nanotechnology and Advanced Materials, Bar-Ilan University, Ramat-Gan 52900, Israel, [2]Brookhaven National Laboratory, Upton, New York 11973-5000, USA. *e-mail: ph89@mail.biu.ac.il

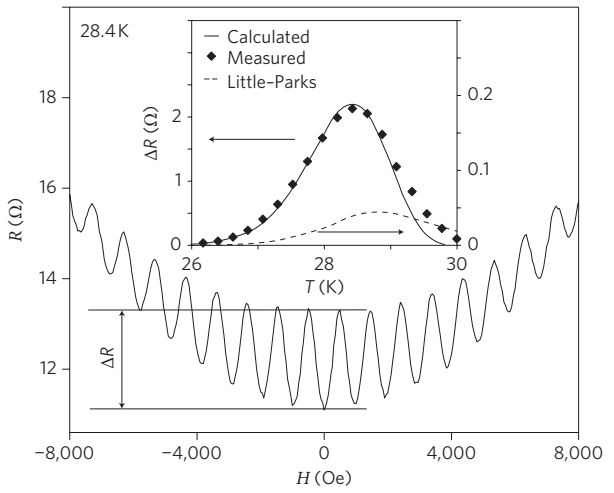

Figure 2 | Magnetoresistance oscillations. Resistance of the $La_{1.84}Sr_{0.16}CuO_4$ network shown in Fig. 1 as a function of applied magnetic field, measured at 28.4 K. The oscillations are superimposed on a parabolic-like background. The amplitude of the oscillations, ΔR, is well defined at low fields. Inset: ΔR as a function of temperature; the solid line is a theoretical fit based on equation (5). The dashed line is an upper limit for the amplitude of resistance oscillations calculated for the Little–Parks effect (right axis; note that the scale on this axis is expanded tenfold).

of $\xi_0 = 2$ nm, the measured critical temperature at zero field $T_c^{onset} = 30.2$ K, and the loop effective radius $r = a/\sqrt{\pi} = 83.5$ nm ($a = 150$ nm is the loop side length), one would expect to find oscillations in T_c with an amplitude $\Delta T_c = 0.14T_c(\xi_0/r)^2 \approx 2.4$ mK (refs 8,12,13,15,16) . This value of ΔT_c yields an upper limit to the resistance amplitude, $\Delta R = \Delta T_c(dR/dT)$, depicted by the dashed line in the inset to Fig. 2, the maximum value of which is a factor of ~50 smaller than the measurement from our experiment.

Given that the Little–Parks effect cannot explain the observed large magnetoresistance oscillations, we suggest that the origin of this phenomenon is the drastically modified vortex dynamics in the patterned film. Although in continuous films the activation energy for vortex creep usually decreases monotonically with the applied magnetic field[19–21], in nanopatterned films this activation energy becomes oscillatory, as moving vortices interact with the current induced in the nanoloops, which is a periodic function of the field strength. Periodicity of the induced current results directly from the fluxoid quantization[12,13,15,22], which is also the source of the Little–Parks effect. The fluxoid, consisting of the flux induced by the supercurrent in the loop and by the external magnetic field, is characterized by the quantum vorticity number N, which defines the energy state of the superconducting loop. In the lowest energy state, N is equal to H/H_0 rounded to the nearest integer[15,16].

Thermal excitation of vortices causes fluxoid transitions from the equilibrium quantum state N to a higher energy state. Other groups[23,24], in their analysis of magnetic scanning microscope measurements of a mesoscopic superconducting ring, have calculated the energies $\Delta E_{in}^{\pm}$ and $\Delta E_{out}^{\pm}$ required to create a vortex (+) or an antivortex (−) and carry it into or outside of the superconducting loop, respectively:

$$\Delta E_{in}^{\pm} = \Delta E_{out}^{\pm} = E_v + E_0[\pm(N - H/H_0) + 1/4] \qquad (1)$$

The first term in equation (1), $E_v = (\Phi_0^2/(8\pi^2\Lambda(T)))\ln(2w/(\pi\xi(T)))$, is field-independent and represents the energy needed for the creation of the vortex/antivortex in the superconducting wire. Here, w is the wire width, $\xi(T) = 0.74\xi_0(1-T/T_c)^{-1/2}$ is the Ginzburg–Landau coherence length[16], and $\Lambda(T) = 2\lambda(T)^2/d$ is the Pearl penetration depth[16,25] in a film of thickness d and with a London penetration depth $\lambda(T) = \lambda_0(1-(T/T_c)^2)^{-1/2}$. The second term in equation (1) is periodic with the field, expressing the interaction of a vortex or an antivortex with the current associated with the fluxoid in terms of the energy, $E_0 = (\Phi_0^2/(8\pi^2\Lambda(T)))(w/a)$. Note that equation (1) is valid in the limit of large penetration depth, $\Lambda \gg w$, and for narrow rings with widths much smaller than the radius of the loops, r. Nevertheless, the width has to be sufficiently large to accommodate a vortex[26]. The quantized values of N lead to periodically oscillating values of $(N-H/H_0)$.

In the following we consider fluxoid transitions accomplished by only one vortex or antivortex entry and exit. Thermodynamic averaging of these four types of excitation energies, ΔE_i, yields an effective potential barrier ΔE_{eff}:

$$\Delta E_{eff} = \sum \Delta E_i e^{-\Delta E_i/k_B T} / \sum e^{-\Delta E_i/k_B T} \qquad (2)$$

By inserting equation (1) for ΔE_i, one obtains

$$\Delta E_{eff} \approx (E_v + E_0/4) - E_0^2(N-H/H_0)^2/k_B T \qquad (3)$$

which includes a field-independent term and a term periodic with the field.

We derive the magnetoresistance by applying Tinkham's approach in analysing the broadening of the resistive transition in high-T_c superconductors[20]. Replacing the activation energy in his equations with ΔE_{eff} given in equation (3), yields

$$\frac{R}{R_n} = \left[I_0\left(\frac{\Delta E_{eff}}{2k_B T}\right)\right]^{-2} \qquad (4)$$

where I_0 is the zero-order modified Bessel function of the first kind. Equation (4) describes a periodic function with period $H_0 = \Phi_0/A$ and temperature-dependent amplitude

$$\Delta R \approx R_n\left(\frac{E_0}{2k_B T}\right)^2 \frac{I_1(\alpha)}{(I_0(\alpha))^3} \qquad (5)$$

where $\alpha = (E_v + E_0/4)/(2k_B T)$, and I_1 is the first-order modified Bessel function of the first kind. Note that E_v and E_0 are a function of the two length scales, λ_0 and ξ_0, which can be used as fitting parameters for the measured temperature dependence of the amplitude of the oscillations. The fit shown by the solid line in the inset to Fig. 2 yields $\lambda_0 = 750$ nm and $\xi_0 = 2.4$ nm. Note that these values of λ_0 and ξ_0 may be influenced by the lithographic process, which may cause damage in regions near the surfaces, thus making the effective thickness and width significantly smaller than the nominal values.

Figure 3b presents calculation of $R(H,T)/R_n$ based on equation (4) and using the above values for λ_0 and ξ_0. The calculated $R(H,T)$ is similar to the experimental results (Fig. 3a) in low magnetic fields where the parabolic-like background on which the oscillations are superimposed is negligible (see Fig. 2). Extension of this analysis to also describe the background arising at higher fields requires modification of equation (1) to include field-dependent terms of higher order[24]. Comparing the details of the experimental and calculated waveforms shown in Fig. 3a and b, one notices that the experimental resistance oscillations look rather sinusoidal, whereas the calculated results exhibit a 'scallop' shape with sharper curvature at the top than at the bottom. This difference is most likely related to the distribution of the size of the fabricated loops.

We note that equation (4) can also explain the broadening of $R(H=0,T)$ in the patterned film as shown in the inset to Fig. 1. In zero field, R depends only on the non-periodic part, E_v, in

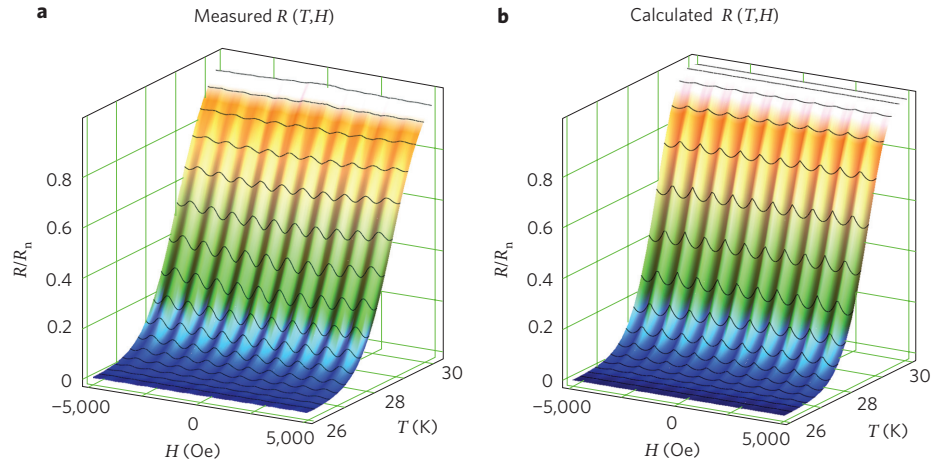

Figure 3 | Comparison of measured and calculated magnetoresitance oscillations. a, Measured normalized resistance of the network shown in Fig. 1 as a function of the applied magnetic field and temperature. **b**, Normalized resistance calculated using equation (4) for wire width $w = 25$ nm, film thickness $d = 26$ nm, zero-temperature penetration depth $\lambda_0 = 750$ nm and coherence length $\xi_0 = 2.4$ nm. The calculation was made for circular loops of the same area as the square loops: that is, with an effective radius $r = a/\sqrt{\pi} = 83.5$ nm ($a = 150$ nm is the actual loop side length). The values for λ_0 and ξ_0 are obtained from the fit of equation (5) to the temperature dependence of the amplitude shown in the inset to Fig. 2. The colour changes from blue to green to orange to white as the resistance increases from zero to the normal-state value.

equation (3), which decreases as the wire width w is reduced. This allows for easier excitations of vortices and antivortices at lower temperatures, giving rise to non-zero resistance.

In general, magnetoresistance oscillations originate from both the Little–Parks effect and the modified vortex dynamics reported here. However, in high-T_c superconductors, the contribution of the Little–Parks effect is relatively small because of the short coherence length[21], and the contribution of the vortex dynamics is large because of strong thermal fluctuations[27]. It should be mentioned that large-amplitude magnetoresistance oscillations have previously been observed in a different nanostructure made of two low-T_c superconducting nanowires. These oscillations were attributed to the field-driven modulation of barrier heights for phase slips[28,29].

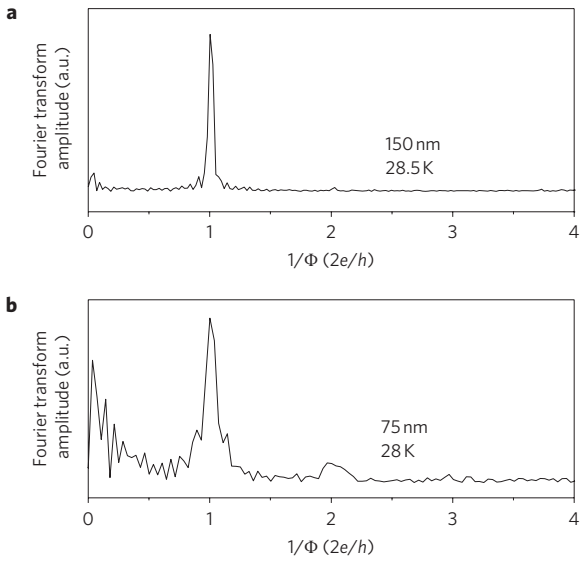

Figure 4 | Periodicity of the magnetoresistance oscillations. a,**b**, Amplitude of the Fourier transform of the magnetoresistance oscillations versus inverse magnetic flux in the 150-nm loops at 28.5 K (**a**) and the 75-nm loops at 28 K (**b**). The $h/2e$ periodicity is apparent, but the h/e periodicity is absent, and the $h/4e$ periodicity appears as the second harmonic of the $h/2e$ fundamental component.

As that interpretation relates to the one-dimensional superconducting wires ($w < \xi$), it may not be directly applicable to our high-T_c loops in which the wire width is an order of magnitude larger than the coherence length.

Recent theoretical studies[1–6] predicted that the magnetoresistance in high-T_c superconducting nanorings with a d-wave order-parameter should show an additional component with flux periodicity h/e. This component is expected even for loops of length scales larger than the coherence length. Figure 4 shows the Fourier transform analysis of magnetoresistance oscillations for both the 75- and 150-nm loops. Evidently, despite the enhanced magnetoresistance oscillations observed in our experiment, a periodicity of h/e is not observed, even in the 75-nm loops (which are the smallest prepared so far with high-T_c superconductors).

More recently, a periodicity of $h/4e$ (corresponding to half a quantum of flux) was predicted for striped high-T_c superconductors, replacing the usual periodicity of $h/2e$ (which corresponds to a quantum of flux[7]). As is evident from Fig. 4, in our optimally doped $La_{1.84}Sr_{0.16}CuO_4$ films, the $h/4e$ flux periodicity does not replace the $h/2e$ periodicity, but only appears as its second harmonic.

In summary, the resistance of a network of nanoscale loops of $La_{1.84}Sr_{0.16}CuO_4$ oscillates as a function of the magnetic flux through the loops in a way that cannot be explained by the classic Little–Parks effect. These oscillations are rather attributed to the field-driven modulation of the height of the energy barrier to vortex motion. The absence of h/e and $h/4e$ periodicities in these oscillations is at variance with some recent theoretical predictions[1–7] for this type of system. However, efforts to discover such periodicities should continue by extending this work to higher and lower doping across the entire phase diagram.

Methods

The $La_{1.84}Sr_{0.16}CuO_4$ films were synthesized by MBE and spin-coated with poly(methyl methacrylate) (PMMA) electron-beam resist with a molecular weight of 495,000, diluted with anisole, providing a thickness of 180 nm after 1 min of spinning at 4,000 rpm. The samples coated with PMMA were subsequently baked for 90 s on a hotplate at 100 °C. The desired network pattern was exposed in the PMMA layer using a CRESTEC CABLE-9000C high-resolution electron-beam lithography system. The PMMA was used as a negative electron-beam resist; note that when PMMA is exposed to a sufficiently high electron dose it crosslinks[30] and becomes insoluble in most organic solvents. After removing the unexposed PMMA using methyl isobutyl ketone (MIBK), a mask was formed that defined the desired

network pattern (Fig. 1, main panel). This pattern was then transferred to the superconducting film by removing the uncovered parts of film using a standard argon ion milling process. The result of this last step is shown in the left inset to Fig. 1.

The network resistance was measured using a Quantum Design Physical Properties System over temperatures from 2 to 300 K with a stability of about $\pm$0.001 K, and in magnetic fields of up to 9 T. A four-point contact resistance configuration was used, in which a d.c. current of 1 μA was fed through two relatively large current leads placed on opposite sides of the network and the d.c. voltage was measured across an additional two leads. All four leads were made from the same $La_{1.84}Sr_{0.16}CuO_4$ superconducting film as a continuous part of the network to avoid undesirable metal/superconductor contact effects.

Received 1 March 2010; accepted 10 May 2010; published online 13 June 2010

References

1. Barash, Y. S. Low-energy subgap states and the magnetic flux periodicity in *d*-wave superconducting rings. *Phys. Rev. Lett.* **100,** 177003 (2008).
2. Juricic, V., Herbut, I. F. & Tesanovic, Z. Restoration of the magnetic *hc*/*e*-periodicity in unconventional superconductors. *Phys. Rev. Lett.* **100,** 187006 (2008).
3. Loder, F. *et al.* Magnetic flux periodicity of *h*/*e* in superconducting loops. *Nature Phys.* **4,** 112–115 (2008).
4. Vakaryuk, V. Universal mechanism for breaking the *hc*/*2e* periodicity of flux-induced oscillations in small superconducting rings. *Phys. Rev. Lett.* **101,** 167002 (2008).
5. Wei, T.-C. & Goldbart, P. M. Emergence of *h*/*e*-period oscillations in the critical temperature of small superconducting rings threaded by magnetic flux. *Phys. Rev. B* **77,** 224512 (2008).
6. Zhu, J.-X. & Quan, H. T. Magnetic flux periodicity in a hollow *d*-wave superconducting cylinder. *Phys. Rev. B* **81,** 054521 (2010).
7. Berg, E., Fradkin, E. & Kivelson, S. A. Charge-*4e* superconductivity from pair-density-wave order in certain high-temperature superconductors. *Nature Phys.* **5,** 830–833 (2009).
8. Gammel, P. L., Polakos, P. A., Rice, C. E., Harriott, L. R. & Bishop, D. J. Little–Parks oscillations of T_c in patterned microstructures of the oxide superconductor $YBa_2Cu_3O_7$: experimental limits on fractional-statistics-particle theories. *Phys. Rev. B* **41,** 2593–2596 (1990).
9. Castellanos, A., Wordenweber, R., Ockenfuss, G., Hart, A. v. d. & Keck, K. Preparation of regular arrays of antidots in $YBa_2Cu_3O_7$ thin films and observation of vortex lattice matching effects. *Appl. Phys. Lett.* **71,** 962–964 (1997).
10. Crisan, A. *et al.* Anisotropic vortex channeling in $YBa_2Cu_3O_{7+\delta}$ thin films with ordered antidot arrays. *Phys. Rev. B* **71,** 144504 (2005).
11. Ooi, S., Mochiku, T., Yu, S., Sadki, E. S. & Hirata, K. Matching effect of vortex lattice in $Bi_2Sr_2CaCu_2O_{8+y}$ with artificial periodic defects. *Physica C* **426–431,** 113–117 (2005).
12. Little, W. A. & Parks, R. D. Observation of quantum periodicity in the transition temperature of a superconducting cylinder. *Phys. Rev. Lett.* **9,** 9–12 (1962).
13. Parks, R. D. & Little, W. A. Fluxoid quantization in a multiply-connected superconductor. *Phys. Rev. A* **133,** 97–103 (1964).
14. Mooij, J. E. & Schön, G. B. J. (eds) Proc. NATO Workshop on Coherence in Superconducting Networks. *Physica. B* **152,** 1–302 (1988).
15. Tinkham, M. Consequences of fluxoid quantization in the transitions of superconducting films. *Rev. Mod. Phys.* **36,** 268–276 (1964).
16. Tinkham, M. *Introduction to Superconductivity* (McGraw-Hill, 1996).
17. Koshnick, N. C., Bluhm, H., Huber, M. E. & Moler, K. A. Fluctuation superconductivity in mesoscopic aluminum rings. *Science* **318,** 1440–1443 (2007).
18. Wen, H. H. *et al.* Hole doping dependence of the coherence length in $La_{2+x}Sr_xCuO_4$ thin films. *Europhys. Lett.* **64,** 790–796 (2003).
19. Yeshurun, Y., Malozemoff, A. P. & Shaulov, A. Magnetic relaxation in high-temperature superconductors. *Rev. Mod. Phys.* **68,** 911–949 (1996).
20. Tinkham, M. Resistive transition of high-temperature superconductors. *Phys. Rev. Lett.* **61,** 1658–1661 (1988).
21. Blatter, G., Feigel'man, M. V., Geshkenbein, V. B., Larkin, A. I. & Vinokur, V. M. Vortices in high-temperature superconductors. *Rev. Mod. Phys.* **66,** 1125–1388 (1994).
22. London, F. On the problem of the molecular theory of superconductivity. *Phys. Rev.* **74,** 562–573 (1948).
23. Kirtley, J. R. *et al.* Fluxoid dynamics in superconducting thin film rings. *Phys. Rev. B* **68,** 214505 (2003).
24. Kogan, V. G., Clem, J. R. & Mints, R. G. Properties of mesoscopic superconducting thin-film rings: London approach. *Phys. Rev. B* **69,** 064516 (2004).
25. Pearl, J. Current distribution in superconducting films carrying quantized fluxoids. *Appl. Phys. Lett.* **5,** 65–66 (1964).
26. Qiu, C. & Qian, T. Numerical study of the phase slip in two-dimensional superconducting strips. *Phys. Rev. B* **77,** 174517 (2008).
27. Yeshurun, Y. & Malozemoff, A. P. Giant flux creep and irreversibility in an Y-Ba-Cu-O crystal: an alternative to the superconducting-glass model. *Phys. Rev. Lett.* **60,** 2202–2205 (1988).
28. Hopkins, D. S., Pekker, D., Goldbart, P. M. & Bezryadin, A. Quantum interference device made by DNA templating of superconducting nanowires. *Science* **308,** 1762–1765 (2005).
29. Pekker, D., Bezryadin, A., Hopkins, D. S. & Goldbart, P. M. Operation of a superconducting nanowire quantum interference device with mesoscopic leads. *Phys. Rev. B* **72,** 104517 (2005).
30. Hoole, A. C. F., Welland, M. E. & Broers, A. N. Negative PMMA as a high-resolution resist—the limits and possibilities. *Semicond. Sci. Technol.* **12,** 1166–1170 (1997).

Acknowledgements

The authors thank A. Frydman, B. Ya. Shapira, B. Rosenstein, E. Zeldov, Y. Oreg, O. Pelleg, A. Bollinger, A. Gozar, Z. Radović and V. Vinokur for helpful discussions. Y.Y. and A.S. acknowledge support of the Deutsche Forschungsgemeinschaft through the Deutsch–Israelische Projektkooperation (grant no. 563363). I.S. thanks the Israeli Ministry of Science and Technology for an Eshkol scholarship. The work at BNL was supported by the US Department of Energy (contract no. MA-509-MACA).

Author contributions

G.L and I.B. synthesized and characterized the superconducting films. I.S. designed and made the patterns, performed the magnetoresistance measurements and analysed the data. All authors contributed to the theoretical interpretation and were involved in the completion of the manuscript.

Additional information

The authors declare no competing financial interests. Reprints and permission information is available online at http://npg.nature.com/reprintsandpermissions/. Correspondence and requests for materials should be addressed to I.S.